Int J Pharm Bio Sci 2014 July ; 5 (3) : (B) 533 - 542

Research Article **Biochemistry**

International Journal of Pharma and Bio Sciences **ISSN 0975-6299**

SYNTHESIS AND CHARACTERIZATION OF FUNCTIONALIZED SUPERPARAMAGNETIC NANOPARTICLES FOR ISOLATION OF DNA

A. P. TIWARI, S. J.GHOSH AND S.H PAWAR*

Center for Interdisciplinary Research, D.Y. Patil University, Kolhapur - 416006, MS, India.

ABSTRACT

Iron oxide nanoparticles were synthesized and coated with silica by conventional co-precipitation method. Silica coated iron oxide nanoparticles were surface functionalized with chitosan. Silica coating and chitosan functionalization were confirmed by FTIR and TG-DTA analysis. XRD pattern revealed that the pure phase of Fe_3O_4 was retained even after coating. Particles of average size 12 nm were obtained as revealed in TEM images. The chitosan functionalized Fe_3O_4@Silica superparamagnetic nanoparticles show a saturation magnetization as high as 56emu/g and enriched rapidly under external magnetic field. The results point out the prospective of these nanoparticles to be used as adsorbent and desorbent of negatively charged DNA. The nanoparticles were successfully exploited for purification of DNA from *Escherichia coli* bacterial culture. The A_{260}/A_{280} value of eluted DNA was close to 1.8, indicating that the isolated DNA is relatively pure and without RNA and protein contamination. The whole process relied on an instrument free "green chemistry" approach and eliminates the need of toxic chemicals.

KEYWORDS: DNA isolation, Magnetic separation, Chitosan, superparamagnetic nanoparticles, Fe_3O_4@Silica.

S.H PAWAR
Center for Interdisciplinary Research, D.Y. Patil University, Kolhapur - 416006, MS, India.

1. INTRODUCTION

Completion of Human genome project in April 2003 brought a new upheaval in the field of genetics. The role of DNA sequences as a basic unit of heredity and its association with genetic diseases was established[1]. Since then many conventional DNA isolation protocol has been designed and practiced[2]. Most of them rely on toxic reagents and use shearing processes like centrifugation which hinders the quality of DNA to be used in downstream application. Consequently, the necessity of developing of cost effective and non toxic methods for isolation of high quality DNA is in demand which can replace traditional methods that usually make use of toxic reagents[3]. The surface modified magnetic nanoparticles may provide an alternative way for DNA isolation. They have emerged as a promising candidate for various biomedical applications such as in separation and purification of biomolecules and cells[4], targeted drug delivery[5], gene delivery[6], in hyperthermia[7] and in biosensors[8]. These magnetic adsorbents make the entire process of isolation and purification, simple and automated owing to their physical properties like nanosize, high magnetization and specificity in binding to special targets.[9] The organic and inorganic polymer coated magnetite composites have been utilized for isolating nucleic acids. Silica-coated magnetic beads[10], polyethylenimine based magnetic beads[11], and methacrylate-based polymer microspheres[12] were the typical examples. It is worthy to note that some natural polysaccharide, such as dextran[13] and chitosan[14] may be competitive for modifying the magnetic particles for isolation of DNA. Coating of polymers over magnetic nanoparticles induces inter-particle repulsion and thereby lowers the magnetic attraction between particles which prevent them from agglomeration when an external field is applied.[15] Among the magnetic materials, amino group functionalized magnetic nanoparticles are of great interest because of their superparamagnetism nature, biocompatibility, and facile surface modification. Amino groups on the surface of magnetic composites can be easily activated for covalent coupling with various ligands suitable for specific interaction with biological molecules.[16] Well regulated positive amino group of chitosan along with excellent biocompatibility makes it an appropriate candidate for DNA adsorption[14]. Duplex DNA possesses two univalent negative charges per base pair at wide range of solution pH, whereas magnetic nanoparticles functionalized with amino groups are positively charged in acidic and near neutral solutions. Therefore, the combination of two oppositely charged components can often occur through electrostatic coupling and hydrophobic interactions. Role of temperature and ionic strength has also been previously investigated in isolation and purification of biomoloecules.[11, 17.] Recently, both silica and chitosan have been exploited widely as surface adsorbents and used in various researches including those of DNA isolation from Bacterial culture.[18, 19] In the present study, highly superparamagnetic, chitosan functionalized Fe_3O_4@Silica nanoparticles were synthesized and its surface properties were optimized for DNA purification from bacterial culture .To the best of our knowledge, this is the first reporting on use of the novel chitosan functionalized Fe_3O_4@Silica nanoparticles as an adsorbent for purification of bacterial DNA. An instrument free green approach of DNA purification has been presented and is suitable for both small as well as large scale DNA purification. This method is expected to offer an alternative for on-site and rapid large scale DNA purification.

2. EXPERIMENTAL

2.1. Materials

Analytical grade chemicals were used for preparation of chitosan functionalized Fe_3O_4@Silica nanoparticles and isolation of DNA. Iron(II) chloride tetra hydrate, polyethylene glycol (PEG, M_W = 6000), sodium chloride (NaCl), Tris-HCl, ethylene diamine tetraacetic acid (EDTA), sodium dodecyl sulphate (SDS), sodium hydroxide (NaOH), hydrochloric acid (HCl), Chitosan (CS, degree of acetylation = 90%) were

purchased from sigma Aldrich chemicals. *E.coli* (ATCC 25922 strain) was used for bacterial DNA purification. All reagents were prepared under aseptic conditions and using double distilled water.

2.2 Synthesis of Chitosan functionalized Fe_3O_4@Silica nanoparticles

Fe_3O_4 nanoparticles were synthesized by alkaline precipitation method as per previously reported method [20]. To be brief, $FeCl_2$ was dissolved in HCl and then NaOH was added to it drop wise under continuous stirring. The appearance of black precipitate indicated the formation of iron oxide nanoparticles. The precipitate was magnetically separated and washed thoroughly with water.The synthesized Fe_3O_4 nanoparticles were silica coated with an acid catalyzed sol-gel reaction. Magnetic suspension (0.1 gm/10 mL Fe_3O_4) was ultrasonically dispersed in a round bottomed flask. Acid catalysis was done by adding 0.1 mL of HCl vigorously. After one hour, 3 mL of water, 5 mL of ammonium hydroxide and 3 mL of TEOS was added to the flask in 5 mL of methanol. The hydrolysis of TEOS were carried out for 7 h at 80 ºC under continuous stirring at 550 rpm. The resultant product was separated by an external magnet and washed thoroughly with double distilled water thrice. [21] Silica coated Fe_3O_4 nanoparticles (0.2 g) were dispersed in 7.5 mL of chitosan solution (4 mg/mL chitosan dissolved in 2 % acetic acid). Suspension was mixed by sonication for 30 min. Finally, the chitosan functionalized silica coated Fe_3O_4 nanoparticles were dried at room temperature.

2.6 Characterization

X-ray diffraction (XRD) patterns were recorded on a Rigaku D/MAXIIA diffractometer using Cu Kα radiation (λ = 1.5406ºA), operating at 40 kV and 40 mA in the 2θ range from 20º to 80º. The crystallite size of the as-synthesized product was estimated from the full-width at half-maximum (FWHM) of the strongest diffraction peak using the Scherer's formula [22].

$$D = 0.9\lambda/\beta \cos\theta$$

Where D is the crystalline size, λ is the wavelength of Cu-Kα radiation, β is FWHM and θ is the diffraction angle of the strongest characteristic peak. Fourier transform infrared (FTIR) spectra were collected on Alpha ATR Bruker (EcoModel) at range of 500-4000 cm^{-1}. Room temperature magnetic moment of the sample was done by Quantum design squid vibrating sample magnetometer (VSM). Thermal properties were recorded by the Trans-analytical instrument (SDT 2960) operated in temperature 35–1000 °C with a heating rate of 10 °C in a N_2 atmosphere to investigate the nature of coating on the particle surface. PSS/NICOMP 380 ZLS particle sizing system (Santa Barbara, CA, USA) with a red He–Ne laser diode at 632.8 ºA in affixed angle 90° plastic cell was used for the measurement of surface charge and colloidal stability. UV visible spectroscopic measurements were taken on UV-1800 Shimadzu, Germany with deuteron and tungsten lamp. The purity of the DNA sample was measured by A_{260} /A_{280} ratio as obtained from U V absorbance study. The concentration of DNA in sample was calculated using formula

C=A / (e*l)

Where, C is the concentration of the nucleic acid, in µg / mL, A is Absorbance at 260 nm, l is width (1cm) and e is extinction coefficient (1 OD_{260} Unit = 50 µg/ mL for double stranded DNA).[23]

2.7 Purification of genomic DNA from E.coli ATCC 25922 with chitosan functionalized Fe_3O_4@Silica nanoparticles

E.coli ATCC 25922 was grown at 37 °C for overnight in a 250 mL in 100 mL nutrient broth and incubated at 37°C under shaking conditions. Cell lysis was done using 1 % SDS and 0.2 M NaOH solution (solution I). Isolation of genomic DNA by chitosan functionalized Fe_3O_4@Silica nanoparticles was done by adding the nanoparticles to the lysed bacterial culture. Binding buffer (25 % PEG- 6000 and 2.0 M NaCl) of pH 5.0 was added in the same tube. The suspension was gently mixed by pipetting and held for 80 ◦ C for 8 min. The pellet was rinsed with 750 µL of cold 70% ethanol. The supernatant was removed and residual ethanol was evaporated. The nucleic acids were eluted in TE buffer of pH 8.5. The MNPs were then immobilized with the supernatant being

transferred to DNase RNase free tube. The DNA purity, concentration and yield were measured by UV absorbance study.

3. RESULTS AND DISCUSSION

3.1 Structure, composition and morphology

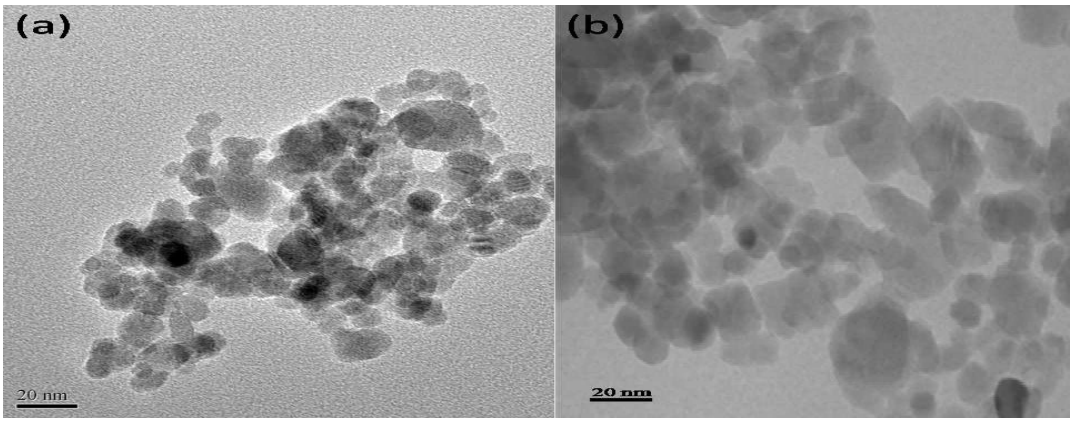

Figure 1
TEM images of (a) bare Fe_3O_4 and (b) chitosan functionalized Fe_3O_4@Silica nanoparticles

Fig.1a illustrates the formation of spherulitic nanoparticulates in an agglomerated form. After functionalization with chitosan the dispersibility of nanoparticles increases (non-aggregated particles) which is evident from Fig. 1b. Improvement in dispersibility after coating with chitosan may be attributed to the presence of the non-magnetic surface layer which readily decreases the interparticle interaction[24]. The average particle size of bare iron oxide nanoparticles is 13 nm (Fig 1a) and chitosan functionalized Fe_3O_4@silica nanoparticles is 17 nm (Fig 1b) which is in accordance with the obtained crystalline size from XRD results.

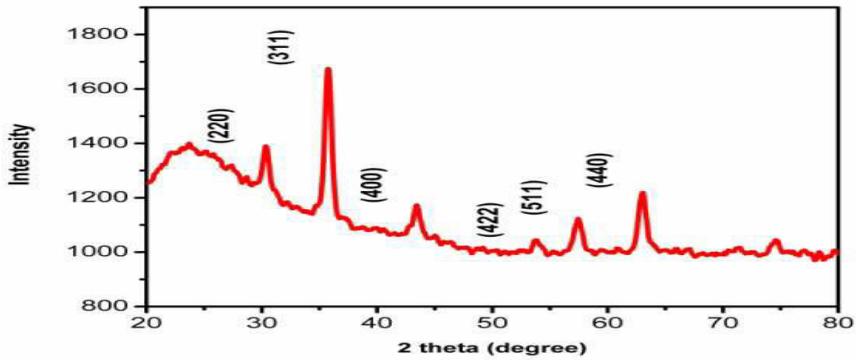

Figure 2
XRD pattern of chitosan functionalized Fe_3O_4@silica nanoparticles.

The XRD pattern of chitosan functionalized Fe_3O_4@Silica is shown in Fig. 2. The characteristic peaks for Fe_3O_4 (2θ = 29.98, 35.46, 43.14, 53.55, 57.20, 62.77) in XRD as marked by their indices (220), (311), (400), (422), (511) and (440) are shown. These are in accordance with standard JCPDS card No. 79-0419. Moreover broadening at 23 is attributed to silica coating[25].The absence of chitosan peak may be attributed to the amorphous nature of chitosan. The crystallite size is 17 nm as calculated Debye Scherer

formula. The results clearly indicate that the Fe_3O_4 nanoparticles in core of chitosan functionalized Fe_3O_4@silica did not change the phase and the results are in accordance with Phadatare *et al* [26].

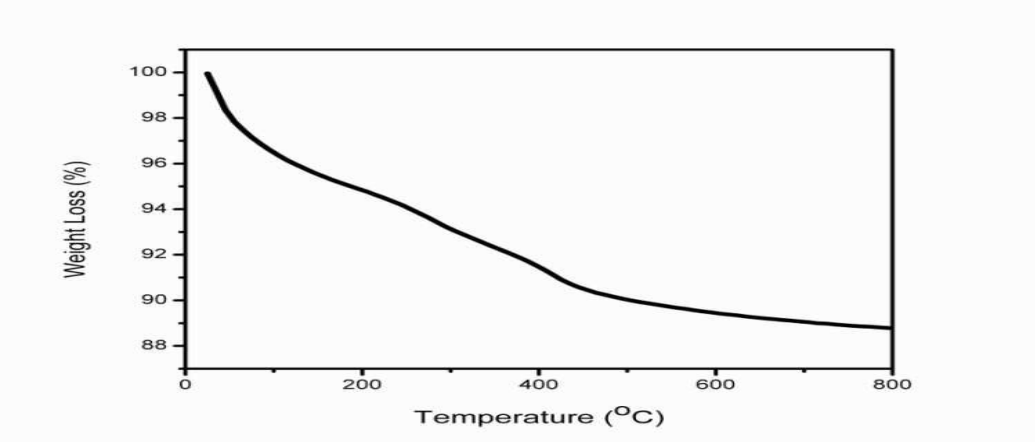

Figure 3
Thermogravimetric analysis of the chitosan functionalized Fe_3O_4 @ silica nanoparticles.

From Fig 3 initial weight loss is observed between 100 ºC and 160 ºC which is attributed with the loss of absorbed water on the surface of chitosan and side product of subsequent condensation of the Si-OH groups. Thermal decomposition is more distinct in the region between 170ºC and 450 ºC concerning to the complex dehydration of the saccharide rings, depolymerization, and decomposition of the acetylated and deacetylated units of the polymer [27]. Hence integration of silica and its interaction with the polymer is revealed. FTIR analysis was carried out in order to verify the silica coating and chitosan functionalization. The spectra for pristine chitosan, silica coated Fe_3O_4 and chitosan functionalized Fe_3O_4@silica nanoparticles is shown in Fig. 4. The peak at 590 cm^{-1} corresponds to Fe-O vibration related to the magnetite phase (Fig. 4a). The adsorption of silica onto surfaces of magnetite particles was confirmed by band at 1078.41cm^{-1} due to Si-O-Si stretching as shown in Fig. 4a[28].The absorption peak at 1646.72 cm^{-1} and 1575.65 cm^{-1} in pristine chitosan spectra are due to absorption by amide I (C=O stretching) and amide II (N-H bending) respectively as shown in Fig. 4c [29].Also absorption peak at 1150 cm^{-1} is due to C-O-C anti symmetric stretching. The complete absence of peak in Fig 4b confirms the participation of this bond in coating. The emergence of two new adsorption peaks at 2920.45 cm^{-1} and 2850.96 cm^{-1} in Fig. 4b attributed to C-H stretching adsorption in chitosan and strongly supports successful coating of chitosan over Fe_3O_4@Silica nanoparticles.

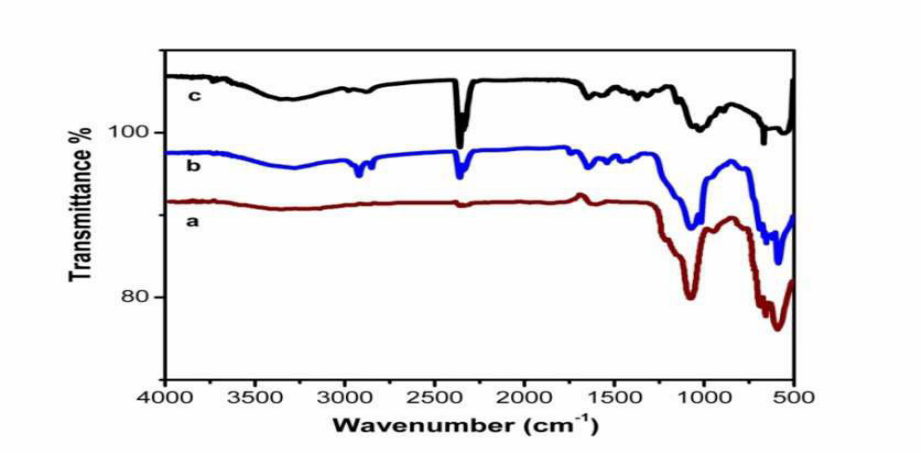

Figure 4
FTIR spectra of (a) silica coated Fe_3O_4 nanoparticles (b) chitosan functionalized Fe_3O_4@silica nanoparticles and (c) pristine chitosan.

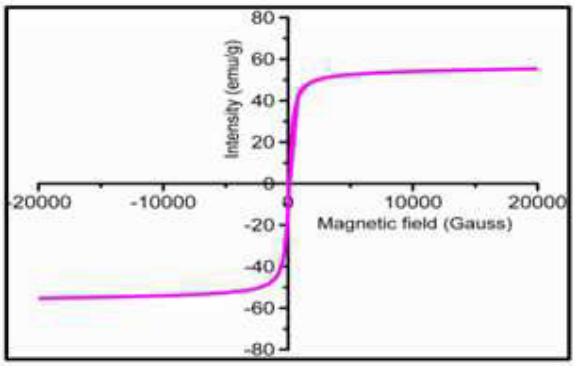

Figure 5
The hysteresis loop of chitosan functionalized Fe_3O_4 @ silica nanoparticles.

It is well known that magnetic particles less than about 30 nm show superparamagnetism[30]. The superparamagnetism properties of magnetic particles were verified by Hysteresis loop measured by VSM. A typical plot of magnetization versus applied magnetic field (M-H loop) at 298 K is shown in Fig 5. The saturation magnetization of the chitosan functionalized Fe_3O_4@Silica nanoparticles is 53.5 emu/g. This large saturation magnetization of magnetic nanoparticles makes them very susceptible to magnetic fields and therefore makes the solid and liquid phases separate easily. The very weak hysteresis loops obtained showed that resultant magnetic nanoparticles were mostly superparamagnetic. The superparamagnetic property of magnetic particles is critical to their application in this field which prevents composite nanoparticles from aggregation and enables them to redisperse rapidly when the magnetic field is removed.

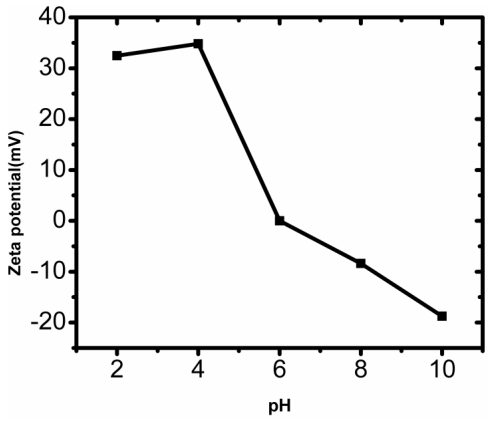

Figure 6
The zeta potentials of chitosan functionalized Fe_3O_4 @ silica nanoparticles suspension at different pH.

Fig.6 shows zeta potential measurements as a function of pH for the chitosan functionalized Fe_3O_4@silica. Zeta potential of nanocomposite suspended in nanopure water was taken at constant ionic strength of 2 M. It is noted that the particles are positively charged at acidic pH with a surface potential of about +35 mV. This confirms the presence of amino groups on the particle surface in their protonated form, which is attributed to the presence of chitosan on the particle surface. At around pH 6.0 the surface potential of nanoparticle decreases to almost 0mV indicating the loss of protonated amino groups. The pKa of chitosan is 6.2, indicating that at or near biological pH half of the amino groups are deprotonated, promoting intramolecular hydrogen bonding and leading to precipitation. From the data given in figure, it is evident that the chitosan modified particles were found to produce a net positive charge at lower pH which is in agreement with the literature. The reason for positive charge is because of the protonation of free amino group present on surface of chitosan modified nanoparticles[31]. At higher pH, that is towards basic the value of Zeta potential changes from positive to negative. The data implied that the nanoparticles could electrostatically bind negatively charged DNA.

3.2 Isolation of DNA by chitosan functionalized Fe_3O_4 @ Silica nanoparticles

The pH induced DNA binding on chitosan functionalized Fe_3O_4 @ Silica nanoparticles was studied. Binding of DNA to the surface of chitosan functionalized Fe_3O_4 @ Silica nanoparticles is due to the electrostatic interaction between positively charged chitosan and negatively charged DNA molecule. DNA is the molecule with a backbone of phosphodiester linkages. Phosphate groups are present in phosphodiester bond, and these are responsible for imparting negative charge to DNA. At neutral pH, theDNA molecule is negatively charged. It is a strong acid with pK_a value less than 1.0. Chitosan; a polycationic molecule has free amino groups at low pH which gives positive charge to molecule. The pK_a of protonated amino groups of chitosan is 6.2. Hence chitosan can hold a positive charge below 6.2 and provide a DNA capture state below 6.2. Hence no binding occurs at pH above 6.2, thus having no positive charge to attract the negative charge[32].

Agarose Gel Electrophoresis

The chitosan functionalized Fe_3O_4 @ Silica nanoparticles were used to purify DNA. Agarose gel electrophoresis was carried out for DNA in four different samples and every eluted sample DNA show a single band at the same position, which indicates that the isolated DNA is very pure .Lane 1 is the molecular weight markers whereas lane 2, lane 3, lane 4, corresponds to different volume of isolated DNA. Lane 5 represents the band pertaining to the DNA isolated by commercially available QIAGEN spin column kit. Table 1 represents the comparison of isolation protocols.It is evident that the chitosan functionalized Fe_3O_4 @ silica nanoparticles are found competitive and took less time than the widely used spin column kit. Moreover the yield of DNA

obtained from 3mL bacterial culture was also higher for the nanoparticles.

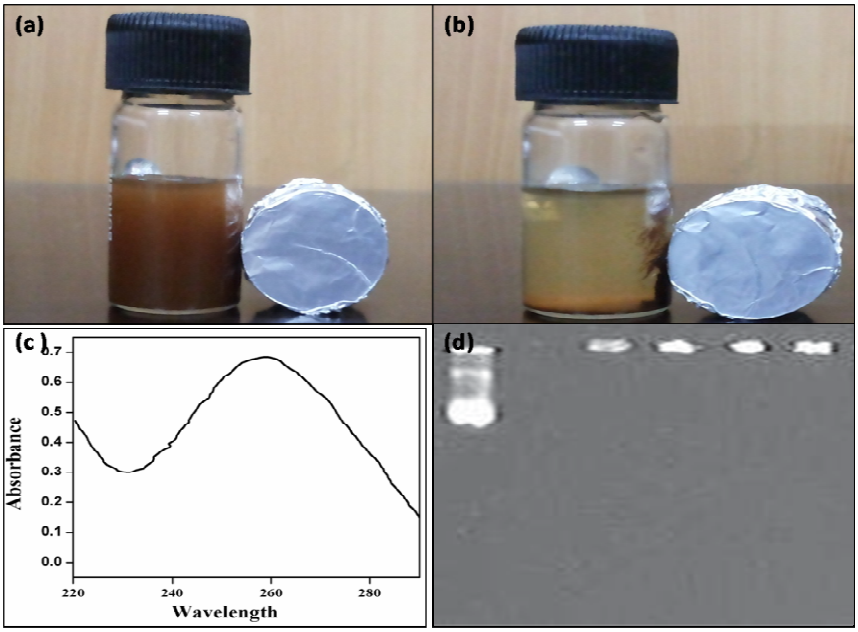

Figure 7

(a) Homogenous suspension of Chitosan functionalized Fe_3O_4@Silica nanoparticles in water, (b) Effect of magnet kept for 10 min,(c) U.V visible spectra of DNA isolated using Chitosan functionalized Fe_3O_4@Silica nanoparticles and (d) Agarose gel electrophoresis pattern of DNA .

Table 1

Comparisons of yield and quality of isolated DNA from Chitosan functionalized Fe_3O_4@silica nanoparticles and with Spin column kits.

	Purity(A_{260}/A_{280})	Yield	Time of isolation
Chitosan functionalized Fe_3O_4@silica nanoparticles	1.85	52µg	8 min
Qiagen spin columns	1.84	21.3µg	12 min

4. CONCLUSION

In summary, chitosan functionalized Fe_3O_4@Silica nanoparticles with high magnetization was successfully synthesized. The nanoparticles are highly stable in colloidal solutions. The prepared composite has the ability to successfully adsorb and desorb DNA from crude bacterial extract. The quality of DNA isolated as assessed by A_{260}/A_{280} is 1.8 which indicates highly pure DNA with no RNA and protein contamination. The proposed instrument free “green chemistry” approach in the present was superior to existing one as the entire method can be accomplished in a single tube without the need of centrifuge and other equipments and hence can be beneficial in underequipped laboratories. Moreover whole isolation protocol was devoid of harmful chemicals and organic solvents hence increase the chance of obtaining good quality DNA. Nanoparticles presented here may find its place in various biomedical applications particularly in increasing the sensitivity of DNA based biosensors. More work is going on to understand the forces behind DNA nanoparticle interaction.

ACKNOWLEDGEMENT

The authors wish to thank for financial assistance of the Department of Science and Technology (DST), New Delhi. Authors are thankful to IIG, Indore for providing VSM analysis. Authors are very grateful to Department of Physics, Shivaji University,

and Kolhapur for giving U.V visible measurements, SAIF Shillong for providing the TEM images.

REFERENCES

1. Peng Chen, Dun Pan, Chunhai Fan, Jianhua Chen, Ke Huang, Dongfang Wang, Honglu Zhang, You Li, Guoyin Feng, Peiji Liang, Lin He and Yongyong Shi ,*Nature Nanotechnology* , 09/2011; 6(10):639-44.
2. R.Prabavathi and V.Mathivanan , *International Journal of Pharma and Bio Sciences* ,Vol 3/Issue 1/Jan – Mar 2012 .
3. R. A. H. Oorschot, K. N. Ballantyne and R. J. Mitchell, *Investigative Genetics*, 2010, 1-14.
4. M. Shao, F. Ning, J. Zhao, M. Wei, D. G. Evans and X. Duan, *J. Am. Chem. Soc.*, 2012, 134, 1071–107.
5. Z. Xu, Y. Feng, X. Liu, M. Guan, C. Zhao and H. Zhang, *Colloids Surf. B*, 2010, 81, 503–507.
6. T. Cheang, B. Tang, A.Xu, G.Chang, Z. Hu, W.He, Z. Xing, J.Xu, M. Wang and S. Wang, *International Journal of Nanomedicine*, 2012, 7, 1061–1067.
7. V.A Karande, R.N.Patil, A.P Tiwari, R.K.Satvekar, A.V.Raut, S.J.Ghosh and S.H.Pawar*, *International Journal of Plant, Animal and Environmental Sciences, 2014, 4, 2*.
8. J. Garcia, Y. Zhang, H. Taylor, O. Cespedes, M. E. Webb and D. Zhou, *Nanoscale*, 2011, 3, 3721–3730.
9. H. J. Chung, C. M. Castro, H. Im, H. Lee and R.Weissleder, *nature nanotechnology* DOI: 10.1038/NNANO.2013.70.
10. Y. Li, J. Church, A.Woodhead and F. Moussa, *Spectrochimica Acta Part A*, 2010, 76, 484–489.
11. Chiang CL, Sung CS, Wu TF, Chen CY and Hsu CY, *J Chromatogr B Analyt Technol Biomed Life Sci*. 2005 Aug 5;822(1-2):54-60.
12. I. Percin, V. Karakoc, S. Akgol, E. Aksoz and A. Denizli, *Materials Science and Engineering: C* , 2012, 32, 1133–1140.
13. J. Li, Y. Zhou, M. Li, N. Xia, Q. Huang, H. Do, Y. Liu, and F. Zhou, *J. Nanosci. Nanotechnol*., 11, 2011,10187-10192.
14. W. Cao, C. J. Easley, J. P. Ferrance and James P. Landers, *Anal. Chem.*, 2006, 78, 7222-7228.
15. V. M. Khot, A. B. Salunkhe, N. D. Thorat,R. S. Ningthoujam and S. H. Pawar,. *Dalton Trans.*, 2013, 42, 1249.
16. L. Gai, X.Han,Y. Hou, J. Chen, H. Jianga and X. Chena, *Dalton Trans*., 2013, 42, 1820.
17. Z. Shan , C. Li , X. Zhang, K. D. Oakes, M. R. Servos, Q. Wua, H. Chen, X. Wang, Q. Huang, Y. Zhou and W. Yang, *Analytical Biochemistry* ,2011,412 , 117–119.
18. K. A. Hagan, W. L. Meier,J. P. Ferrance and J. P. Landers, *Anal. Chem.* 2009, *81,* 5249–5256.
19. R. K. Satvekar, S. S. Rohiwal , A. V. Raut , V. A. Karande, B. M. Tiwale and S. H. Pawar, *Microchim. Acta.*, 2014, 181, 1-2, 71.
20. P.B.Shete, R.M.Patil, R.S.Ningthoujam, S.J Ghosh and S.H. Pawar, 2013, *New J. Chem.*, 2013,37, 3784-3792 .
21. C.L. Chiang, C.S. Sung, C.Y. Chen, *Journal of Magnetism and Magnetic Materials,* 2006,305, 483–490.
22. B. D. Cullity, *Elements of X-Ray Diffraction*, Addison-Wesly Publishing Co. Inc., 1976, ch.14.
23. T. Tanaka, R. Sakai, R. Kobayashi, K. Hatakeyama and T. Matsunaga, *Langmuir*, 2009, 25, 2956–2961.
24. D. Panda, K. Rathinasamy, M. K. Santra and L. Wilson, *Proc. Natl. Acad. Sci. U. S. A*., 2005, 4, 253.
25. D. Shaoa, A. Xiaa , J. Hua, C. Wanga and W. Yub, *Colloids and Surfaces A: Physicochem. Eng. Aspects*, 2008,322, 61–65.
26. M.R. Phadatare , A.B. Salunkhe , V.M. Khot , C.I. Sathish , D.S. Dhawale and S.H. Pawar , *Journal of Alloys and Compounds*,2013, 546 ,314–319.
27. R.K. Satvekar, M.R. Phadatare, V.A. Karande, R.N. Patil, B.M. Tiwale and S.H. Pawar International Journal of Basic and Applied Sciences, 2012, 4, 468-476.

28. F. A. Sagheer and S.Muslim, *Journal of Nanomaterials*, 2010, doi:10.1155/2010/490679.
29. Y. Ren, H. A. Abbood, F. He, H. Peng and K. Huang, *Chemical Engineering Journal*, 2013, 226, 300–311.
30. Z. Teng, J. Li, F. Yan and R. Zhao, W. Yang, *J. Mater. Chem*., 2009, 19, 1811–1815.
31. Y.C. Chang and D.H. Chen, *Journal of Colloid and Interface Science,* 2005, 283,446–451.
32. P. E. Vandeventer, J. S. Lin, T. J. Zwang, A. Nadim, M. S. Johal, and A. Niemz, *J. Phys. Chem. B*, 2012, 116, 5661−5670.